

# Parameterization of GDL Liquid Water Front Propagation and Channel Accumulation for Anode Purge Scheduling in Fuel Cells

Jason B. Siegel and Anna G. Stefanopoulou

**Abstract**—This paper parameterizes the 0-dimensional model of liquid water front evolution associated with: (1) water transport through the membrane, and (2) accumulation and transport of liquid water in the Gas Diffusion Layer (GDL) originally presented in [1]. We add here vapor transport into and out of the channels and liquid water removal from the anode channel during a purge. This completely describes a model for purge scheduling, to avoid anode channel plugging, and to prevent over-drying of the membrane. The model is parameterized using two tunable and one experimentally identified parameter to match the rate of liquid water accumulation in the anode channel that was observed via neutron imaging of an operational 53 cm<sup>2</sup> PEMFC. Simulation results for the GDL and Membrane model augmented with a lumped channel model are presented and compared with measured liquid water values.

## I. INTRODUCTION

Water produced at the cathode catalyst layer can diffuse back to the anode side due to the difference in water concentration across the membrane. When air is used on the cathode, nitrogen permeation through the membrane (MB) leads to the accumulation of inert nitrogen in the anode channel [2], [3]. In the anode channel of a Proton Exchange Membrane Fuel Cell (PEMFC) operating with a Dead-Ended Anode (DEA), the small gas flow velocity, gravity, buoyancy, and channel orientation help establish statistically repeatable and large spatiotemporal variations, allowing for model simplification. Water liquid, water vapor, and nitrogen gas will settle to the bottom of the channel, as illustrated in Fig. 1. These heavier molecules will displace hydrogen from that portion of the cell, leading to voltage loss and carbon corrosion of the catalyst support in the cathode [4]. Therefore, scheduling an occasional purge of the anode volume is necessary to remove the accumulated water and inert gas [5], [6]. The boolean control input  $u$ , shown in Fig. 1, can be used to adjust the purge period and duration based on the measured terminal voltage. Too frequent purging wastes hydrogen and may over dry the membrane leading to decreased cell performance and other degradation issues. Hence, a model-based purge-schedule is highly desirable.

The application of simple hybrid modeling and model predictive control (MPC) techniques for water purge management has been demonstrated [7], but it relied on look-up-tables for many parameters, which vary significantly with op-

eration conditions and therefore can not be easily calibrated. To address the issue of simulating and parameterizing a model with coupled PDEs describing liquid and gas transport through the Gas Diffusion Layer (GDL) of a PEMFC, which exhibit steep moving fronts, we developed a simplified three state switching model which tracks the slowly moving liquid water fronts inside the GDLs and the membrane water content [1].

In this work, we show a parameterization of the model using in-situ measurement of the liquid water distribution inside the fuel cell from neutron imaging [8]. The 0-D GDL and membrane model is then augmented with a lumped volume channel model, similar to [6], [9], to demonstrate the GDL channel interaction and show the complete system behavior for model validation. This additional modeling effort should provide better results when using MPC because channel dynamics are included. In the future, this 0-D GDL/MB model could be augmented with a 1-D channel model to form a 1+0D model capable of capturing the effects of distributed channel conditions on water crossover and nitrogen accumulation rates.

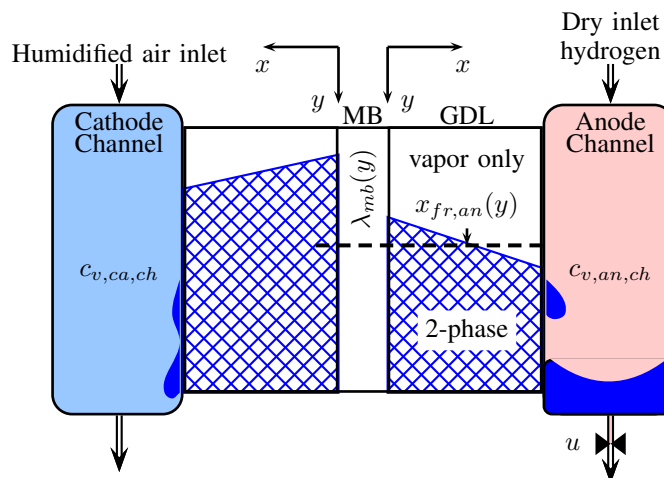


Fig. 1. A schematic of water fronts propagating inside a polymer electrolyte membrane fuel cell. Blue hatched region in the GDL indicates liquid water presence, assumed to be at fixed saturation  $s = s_*$ , or zero. The dashed line indicates the slice the fuel cell GDL/MB shown in Fig. 2.

## II. SYSTEM EQUATIONS 0-D UNIT FUEL CELL MODEL

Liquid water in the GDL is described in terms of liquid saturation  $s = v_l/v_p$ , which is the ratio of liquid volume to open pore volume. Liquid water accumulation in the GDL is modeled using an ODE moving front approach, similar to [10], although here we do not rely solely on the temperature

This work was supported by The National Science Foundation through CBET-0932509

J. B. Siegel is a Graduate Student of Electrical Engineering Systems, and A. G. Stefanopoulou is a Professor of Mechanical Engineering, University of Michigan, Ann Arbor Mi, 48109, USA. siegelj@umich.edu

TABLE I  
NOMENCLATURE

Maximum liquid water flux (mol cm <sup>-2</sup> s <sup>-1</sup> )	$N_{L,max}$
Anode water vapor concentration	$c_{v,an}$
Membrane water content (# H <sub>2</sub> O per SO <sub>3</sub> <sup>-</sup> H <sup>+</sup> )	$\lambda_{mb}$
Vapor flux in the anode GDL (mol cm <sup>-2</sup> s <sup>-1</sup> )	$N_{v,an}$
Water flow from anode GDL to CH (g s <sup>-1</sup> )	$W_{w,an,GDL}$
Liquid saturation in the two phase region	$s_*$
Catalyst layer liquid water saturation	$s_{ctl,j}$
Temperature (K)	$T$
Water activity	$a = c_v/c_{v,sat}$
Faraday's constant	$F$
Current density (A cm <sup>-2</sup> )	$i_{fc}$

gradient, but rather on the hydrophobicity of the GDL, and the capillary pressure gradient to expel water. We assume that the liquid water propagates at a constant, tunable, volume fraction,  $s_*$ , which is slightly larger than the immobile limit. The value  $s_* = 0.37$  was extracted from neutron imaging data of the water accumulation [11].

Water dynamics in the GDL-MB-GDL unit model are governed by the membrane water content and the location of a liquid water front in the GDLs. The membrane water content,  $\lambda_{mb}$ , is calculated from the water flux into the membrane from the cathode side,  $N_{v,ca,mb}$ , and out of the membrane from the anode side,  $N_{v,an,mb}$ ,

$$\frac{d\lambda_{mb}}{dt} = K_{mb}(N_{v,ca,mb} - N_{v,an,mb}), \quad (1)$$

where  $K_{mb} = EW/(\rho_{mb} \delta_{mb})$  is the membrane water uptake rate.

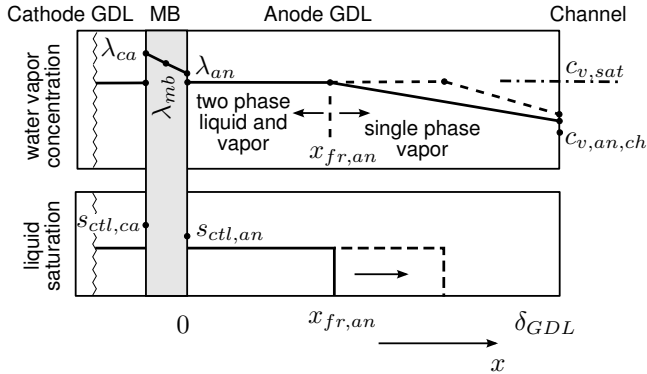


Fig. 2. Two phase water front evolution in the anode GDL for the unit fuel cell model, which represents a 1-D slice from Fig. 1. The advancing two phase front on the anode side GDL, corresponds to mode 2 dynamics. Liquid water fills the GDL up to  $s = s_*$ , then the two phase front propagates toward the channel. Once the front reaches the channel, then liquid begins to accumulate in the channel.

The liquid water front location in the anode GDL,  $x_{fr,an}$ , is governed by the rate of water accumulation in the GDL that is condensing into the liquid phase,  $N_{l,an}$ . Hence the front propagation is given by,

$$\frac{dx_{fr,an}}{dt} = K_L \begin{cases} N_{l,an} & x_{fr,an} < \delta_{GDL} \\ \min(0, N_{l,an}) & x_{fr,an} = \delta_{GDL} \end{cases}, \quad (2)$$

where  $K_L = M_v/(\rho_l s_* \epsilon \delta_{GDL})$  is a constant which accounts for the geometry and density of liquid water in the two

phase region, assuming the front propagates with constant liquid saturation ( $s = s_*$ ), as shown in Fig. 2. The right hand side (RHS) of (2) depends on  $N_{l,an}$ , which is equal to the difference between the flux of water entering the GDL from the membrane,  $N_{v,an,mb}$ , and the flux of vapor leaving from the GDL and entering the channel  $N_{v,an}$ ,

$$N_{l,an} = N_{v,an,mb} - N_{v,an}. \quad (3)$$

For the purpose of tracking the liquid front propagation in the GDL, we can take the gases to be in steady state [12], [10]. We also assume that all the condensation occurs at the membrane-GDL interface (MB-GDL)  $x = 0$ , as proposed in [13], and evaporation at the liquid phase front location  $x = x_{fr,an}$ .

#### A. Membrane Water Transport to Anode

The water flux out of the membrane and into the anode GDL is governed by diffusion and osmotic drag,

$$N_{v,an,mb} = 2 \frac{\alpha_w D_w(\lambda_{mb}, T) \cdot (\lambda_{mb} - \lambda_{an})}{\delta_{mb}} - \frac{n_d i_{fc}}{F}. \quad (4)$$

The first term in (4) describes diffusion in the membrane [14], which is driven by the anode side gradient of the membrane water concentration as it is shown in Fig. 2. The anode water gradient is defined by the state,  $\lambda_{mb}$ , and the water content at the membrane interface with the anode GDL  $\lambda_{an}$ . Since the catalyst layer is very thin, its effect can be lumped into  $\lambda_{an}$ . Therefore, we express  $\lambda_{an}$  as a function of catalyst flooding level,  $s_{ctl,an}$  and the vapor concentration in the GDL  $c_{v,an}(0)$ ,

$$\lambda_{an} = (1 - s_{ctl,an}) \lambda_{T,a} + s_{ctl,an} \lambda_{max}, \quad (5)$$

where  $\lambda_{max} = 22$  is the water content of a liquid equilibrated membrane and  $\lambda_{T,a}$  is the membrane water uptake isotherm [6], [15],

$$\lambda_{T,a} = c_0(T) + c_1(T) a + c_2(T) a^2 + c_3(T) a^3, \quad (6)$$

which is a function of the water activity,  $a$ , at the GDL-MB interface. The water activity in the GDL-MB interface is equal to the ratio of vapor concentration to the saturation value,  $a = c_{v,an}(0)/c_{v,sat}$ . The  $c_i(T)$ ,  $i \in \{0, 1, 2, 3\}$ , values are calculated by a linear interpolation based on temperature between the values at 303 K and 353 K listed in Table II.

The dependence of membrane water content on catalyst liquid saturation is introduced to capture the effect of liquid water in the catalyst layer on membrane water transport [19]. We propose that  $s_{ctl,an}$  be a function of the liquid flux  $N_{l,an}$  as follows,

$$s_{ctl,an} = \frac{\max(N_{l,an}, 0)}{N_{L,max}}, \quad (7)$$

where  $N_{L,max}$  is the maximum liquid water flux the catalyst layer can handle before becoming completely saturated.  $N_{L,max}$  should be inversely proportional to liquid water

TABLE II  
FUEL CELL PARAMETERS.

$\{c_{0,303}, c_{1,303}, c_{2,303}, c_{3,303}\}$	$\{0.043, 17.81, -39.85, 36\}$ [16]
$\{c_{0,353}, c_{1,353}, c_{2,353}, c_{3,353}\}$	$\{0.3, 10.8, -16, 14.1\}$ [17]
$a_w$ (cm <sup>2</sup> s <sup>-1</sup> )	2.72E-5 [15]
$c_f$ (mol cm <sup>-3</sup> )	0.0012
Nitrogen Permeation (mol cm <sup>-1</sup> s <sup>-1</sup> Ba <sup>-1</sup> )	$K_{N_2,perm} = 1.5 \times 10^{-17}$ [2]
Water molar mass (g mol <sup>-1</sup> )	$M_v = 18$
Vapor diffusivity (cm <sup>2</sup> s <sup>-1</sup> )	$D_V = 0.345$
Corrected diffusivity (cm <sup>2</sup> s <sup>-1</sup> )	$D_{v,e}$ [18]
Membrane thickness (cm)	$t_{mb}=0.00254$
Anode channel volume (cm <sup>3</sup> )	$V_{an,ch}=6.5$
Outlet orifice diameter (cm)	$D_h=0.109$
Channel height (cm)	$H_{ch}=0.1$
GDL thickness (cm)	$\delta_{GDL}=0.0420$
GDL porosity	$\epsilon=0.8$

viscosity, therefore we choose the following functional form with an exponential temperature dependence,

$$N_{L,max}(T) = N_{L0} \left( \exp \left[ N_{L1} \left( \frac{1}{303} - \frac{1}{T} \right) \right] \right), \quad (8)$$

where  $N_{L1}$  and  $N_{L0}$  are tunable parameters.

The second term in (4) describes electro-osmotic drag, which pulls water from the anode to the cathode with the conduction of protons through the membrane, and therefore is dependent on the current density,  $i_{fc}$ . The drag coefficient is given by  $n_d = 2.5\lambda_{mb}/\lambda_{max}$  which depends on the membrane water content.

### B. Water exchange with the channel

The two phase front location inside the GDL also determines the rate of vapor and liquid water flux into the channel. When the front location is inside the GDL,  $x_{fr,an} < \delta_{GDL}$ , then the water exchange with the channel is in the vapor phase only. When the front reaches the channel,  $x_{fr,an} = \delta_{GDL}$ , then the mass flow of water from the GDL into the channel is the sum of the liquid and vapor flux

$$W_{w,an,GDL} = A_{fc} M_v \begin{cases} N_{v,an}, & x_{fr,an} < \delta_{GDL} \\ (N_{v,an} + \max(N_{l,an}, 0)), & x_{fr,an} = \delta_{GDL} \end{cases}. \quad (9)$$

The  $\max(\cdot)$  function prevents liquid water in the channel from entering the hydrophobic GDL, since, in the model formulation,  $N_{l,an} < 0$  represents a receding, two phase front inside the GDL.

### III. SYSTEM MODES

The  $\min(\cdot)$  and  $\max(\cdot)$  functions lead to a switched mode system with the following physical interpretation for the resulting modes:

- Mode 1: Vapor only transport in the GDL, when there is no two phase front i.e.  $x_{fr,an} = 0$  and  $N_{l,an} = 0$ .
- Mode 2: The two phase front is advancing,  $N_{l,an} > 0$  and  $x_{fr,an} \geq 0$ .
- Mode 3: The two phase front is receding,  $N_{l,an} \leq 0$  and  $x_{fr,an} > 0$ .

The dynamic equations describing membrane water content and front propagation in the GDL can be represented by one of three possible system modes for each side of the membrane. The overall system has a total of nine system modes, considering the same three modes for the cathode. For simplicity, we assume the cathode to always be in mode 2 when a humidified air inlet is used, due to the additional product water generation at the cathode. In order to identify the tunable parameters  $N_{L1}$  and  $N_{L0}$ , we consider the case when the anode GDL is also in mode 2. When  $x_{fr,an} = \delta_{GDL}$  and the system is in mode 2, the rate of liquid water accumulation in the anode channel, for various combinations of temperature and current density, can be used to identify the tunable parameters. For a derivation of the system modes, and hybrid switching conditions see [1].

### IV. FITTING WATER TRANSPORT PARAMETERS

TABLE III  
TUNED PARAMETERS. \*  $\alpha_w$  WAS NOT TUNED.

$s^*$	0.37	$N_{L0}$	2.3434
$\alpha_w$	1*	$N_{L1}$	3991

The tunable parameters  $N_{L0}$  and  $N_{L1}$  in (8), can be experimentally determined from neutron imaging data by observing the rate of liquid water accumulation in the anode channel during operation of the PEMFC under DEA conditions [8]. Measurement of liquid water accumulation rate in the anode channel is shown in Figure 3. The quasi steady state accumulation rate is calculated from the time evolution of the system and plotted as a function of current density  $i_{st}$  and cell temperature  $T_{st}$  in Figure 4. The fuel cell operating conditions are chosen to maintain as close to uniform channel conditions as possible so that the lumped channel approximation remains valid. Therefore, experimental data with fully humidified cathode inlet gas feeds were used for parameter identification. Under these operating conditions we can assume that the fuel cell model is operating exclusively in mode 2 for both the anode and cathode GDLs whenever liquid water accumulation in the anode channel is observed. Furthermore, once the GDLs are saturated,  $x_{fr,an} = \delta_{GDL}$ , the rate of liquid water accumulation in the anode can be attributed to the rate of water flux through the membrane in mode 2,  $N_{v,an,mb}^{(2)}$ . Under these assumptions,  $c_{v,an,ch} = c_{v,ca,ch} = c_{v,sat}(T_{st})$ , we can solve for the value of membrane water content,  $\lambda = \lambda_{eq}$  in (10), which is an equilibrium point, by solving  $N_{v,an,mb}^{(2)} = N_{v,ca,mb}^{(2)} = N_{v,an,mb,eq}^{(2)}$ . The function  $N_{v,an,mb,eq}^{(2)}(T_{st}, i_{st}, \lambda = \lambda_{eq}, N_{L0}, N_{L1})$ , which is shown in (11), is fit to the measured liquid water accumulation data, using the non-linear least squares curve fitting routine in MATLAB<sup>®</sup>, for the parameters  $N_{L0}$  and  $N_{L1}$ . An analytic expression for the Jacobian matrix is easily calculated, which speeds up the convergence of the parameter fitting. The specific functional form of  $N_{L,max}$ , given in (8), is independent of the tuning procedure, and therefore the model could easily be parameterized using another functional relationship. The

membrane water transport scaling parameter  $\alpha_w$  affects water transport both in two-phase and sub-saturated conditions, but was not tuned since there was not enough data to provide a reliable tuning of this parameter.  $\alpha_w$  is redundant with  $N_{L0}$  over the set of tuned data.

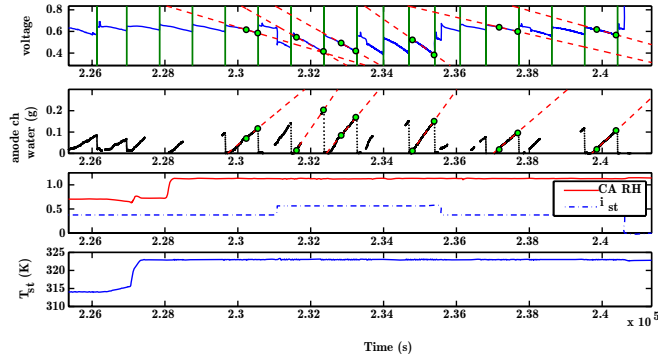


Fig. 3. Extracting anode channel liquid water accumulation rate from neutron imaging data for model tuning.

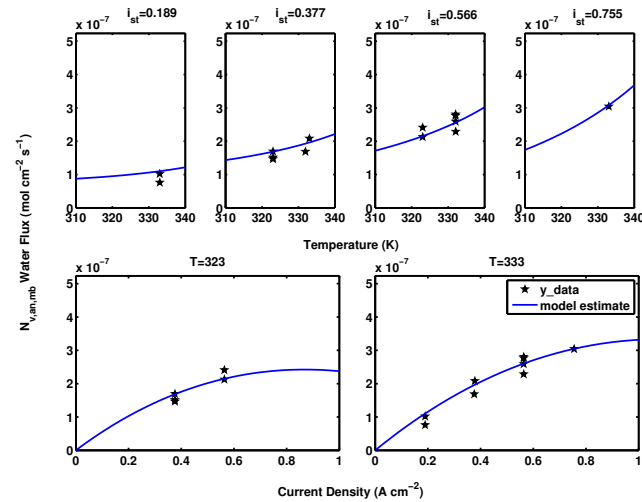


Fig. 4. Fit model, yields a model with convex temp relationship, and concave with current density

The tuned model shows an exponential increase in the rate of water crossover, and hence the liquid accumulation in the anode channel, with increasing temperature due to the exponential term in the diffusion coefficient [14]. The water crossover rate also increases with current density, as the rate of water production increases, until the osmotic drag term begins to dominate (4) at which point the water crossover rate begins to decrease with further increase of current density.

## V. MODEL VALIDATION

In order to perform dynamic validation of the 0-D GDL/MB model, we need to augmented the system equations with a lumped volume channel model to demonstrate the GDL channel interactions and show the complete system behavior. The lumped volume channel equations constitute a mass balance for each of the three constituent gases in the channel volume ( $H_2/O_2$ ,  $N_2$ , and  $H_2O$ ) similar to [6]. The

equations which describe the relationship between pressure drop and mass flow of gas into and out of the cell, Eq. (12), are different from our previous work and chosen to utilize a more numerically stable calculation [20]. The gas flow leaving the anode channel is zero during normal operation. During an anode purge the gas velocity is larger, but still within the laminar flow regime. The lumped channel equation are shown in the Appendix.

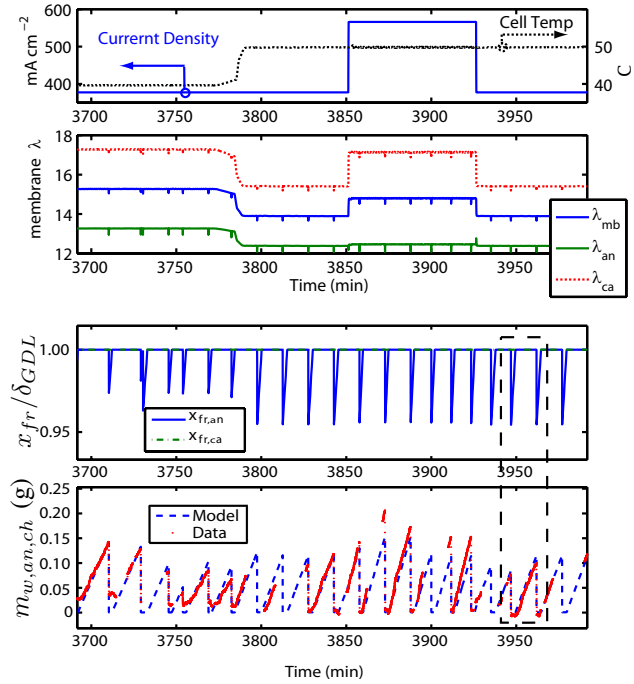


Fig. 5. Simulation of Aug 7, 2007 Experiment at NIST [8]. Cell temperature increased from 314 (K) to 323 (K) at  $t=3785$  (min) (not shown). The model shows good agreement over the range of temperature and current density, but slightly under predicts water transport to the anode at higher current density.

Current density  $i_{st}$ , stack temperature  $T_{st}$ , cathode stoichiometric ratio and cathode inlet relative humidity (dew point temperature) are measured from the experiment and used as the inputs to the hybrid switching model. A simulation of the Aug 7, 2007 Experiment at NIST [8] with a fully saturated cathode inlet feed is shown in Fig. 5. Fig. 5b shows that the anode channel water vapor concentration remains near the saturation value, decreasing only slightly during an anode purge. The membrane water content  $\lambda_{mb}$ , Fig. 5c strongly depends on current density and temperature, increasing with current density at  $t=3850$  (min) and decreasing with temperature at  $t=3785$  (min). The normalized front location is shown in Fig. 5d, and the liquid water mass in the anode channel is shown in the last subfigure.

The anode purges shown in Fig. 6 capture the removal of liquid water from the GDL. This can clearly be seen by the flat sections in the plot of anode channel liquid water mass. Liquid water must completely re-fill the GDL before accumulation of liquid water in the anode channel begins again following an anode purge. The duration of the flat

$$\lambda_{eq} = \frac{4F \lambda_{a=1}(T) N_{L,max}(T) - \lambda_{a=1} i_{fc} + \lambda_{max} i_{fc}}{4F N_{L,max}(T)} \quad (10)$$

$$N_{v,an,mb,eq} = \frac{2 \alpha_w N_{L,max}(T) D_{ve} D_w(\lambda_{eq}, T) (\lambda_{eq} - \lambda_{a=1}(T)) - i_{fc} \delta_{mb} n_d(\lambda_{eq}, T) / F}{(N_{L,max}(T) D_{ve} \delta_{mb} + 2 D_{ve} \alpha_w D_w(\lambda_{eq}, T) (\lambda_{max} - \lambda_{a=1}(T)))} \quad (11)$$

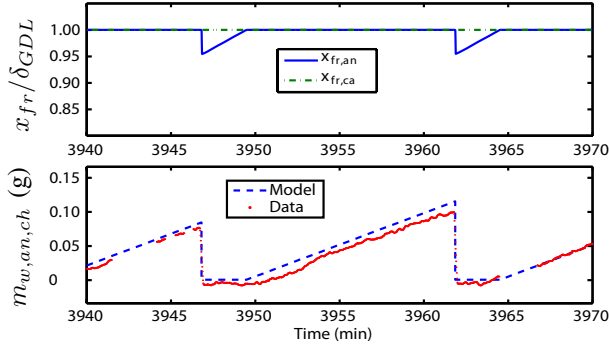


Fig. 6. Same experimental conditions as Figure 11 in [8]. After an anode purge, which removes liquid water from the GDL, liquid water accumulation in the anode channel resumes only after the liquid front reaches back to the channel.

region in the plot of channel liquid water mass depends on the “strength” of the anode purge, both flow rate and duration, and the amount of liquid water present in the channel preceding the purge. Dry hydrogen flowing through the fuel cell must first remove all liquid water from the channel before causing the two phase liquid water front location to recede in the GDL. Our model predicts roughly a 5% change in the anode front location due to the 1 s purge and matches the time period before water accumulation in the channel resumes.

A major limitation of the lumped volume channel model for predicting the net water transport is that the average vapor concentration in the channel is insensitive to changes in cathode inlet RH, due to the saturation caused by the  $\min(\cdot)$  function in (14), and remains fixed at the saturation value ( $c_{v,sat}$ ) until the inlet RH is lowered sufficiently that the water removal rate is higher than the water generation rate. At lower cell temperatures, below 50°C, there may not be sufficient carrying capacity of the air leaving the fuel cell to remove all of the generated water in the vapor phase.

## VI. CONCLUSIONS AND FUTURE WORK

In this paper, a hybrid dynamical model for the advancing and receding two phase liquid-vapor fronts in the GDL of a PEMFC was presented. Three system modes are required to describe the advancing front, receding front, and vapor only phase in the anode GDL. Several simplifying assumptions were presented to describe the slowly evolving liquid water dynamics using ODEs, yielding a reduction in the computational complexity of the model when compared to the traditional approach of solving the coupled two-phase diffusion partial differential equation. The inclusion of catalyst flooding and its resulting impact on membrane water transport highlights another improvement over our

previous work. The model can be used to estimate the membrane water content, the rate of water crossover through the membrane, and liquid water accumulation in the anode channel, all of which impact fuel cell performance.

The 0-D GDL/MB model was parameterized using measurements of liquid water accumulation in the GDL and channels acquired via neutron imaging [8]. The tunable parameters,  $N_{L0}$  and  $N_{L1}$  in (8), were determined using non-linear least squares fitting to the measured water accumulation rate. The parameter  $\alpha_w = 1$  in (4) was not tuned. The value  $s_*$  in (2) was also extracted from the neutron imaging data [11]. Finally, the tuned 0-D GDL/MB model was augmented with a lumped volume channel model and the results are compared with neutron imaging data. The model shows good results for saturated cathode inlet fuel supply. The limitations of the lumped volume channel modeling approach are presented, which explain the lack of model fidelity for sub-saturated inlet conditions.

Our next goal is the development of an along the channel moving front similar to [10], to address the limitations of the lumped channel model and provide better ability to match the measurements of liquid water accumulation in PEMFC when operating with sub-saturated cathode feed gases, so that cathode inlet relative humidity may be considered as an additional control actuator.

## VII. APPENDIX: LUMPED ANODE CHANNEL MODEL

The lumped volume channel equations constitute a mass balance for each of the three constituent gases in the channel volume,

$$\frac{dm_{i,an,ch}}{dt} = W_{i,an,in} + W_{i,an,GDL} - W_{i,an,out}, \quad (13)$$

where  $i \in \{H_2, N_2, w\}$  corresponding to hydrogen, nitrogen, or water. Liquid and vapor are combined into one state in the channel; it is assumed that the channel is at equilibrium. Therefore,

$$m_{v,an,ch} = \min \left( m_{w,an,ch}, \frac{P_{sat}(T_{st}) V_{an,ch} M_v}{R T_{st}} \right), \quad (14)$$

where  $M_v$  is the molar mass of water, and  $P_{sat}(T_{st})$  is the temperature dependent saturated vapor pressure. The remaining water is considered to be in the liquid phase,  $m_{l,an,ch} = m_{w,an,ch} - m_{v,an,ch}$ .

The anode inlet gas flow rate is assumed to be dry hydrogen supply, therefore,  $W_{N_2,an,in} = W_{w,an,in} = 0$  and

$$W_{H_2,an,in} = W_{tot,an,in}, \quad (15)$$

where  $W_{tot,an,in}$  is calculated using Eq. (12), and the anode inlet pressure  $P_{an,in}$ .  $P_{an,in}$  is a constant, since it is set via a pressure regulator.

$$W_{tot} = \begin{cases} A\rho_1 \left( C_{turb} \sqrt{\frac{2}{\rho_1} |P_1 - P_2| + \left( \frac{\nu_1 R_t}{2 C_{turb} D_h} \right)^2} - \frac{\nu_1 R_t}{2 D_h} \right), & \text{if } P_1 \geq P_2 \\ -A\rho_2 \left( C_{turb} \sqrt{\frac{2}{\rho_2} |P_1 - P_2| + \left( \frac{\nu_2 R_t}{2 C_{turb} D_h} \right)^2} - \frac{\nu_2 R_t}{2 D_h} \right), & \text{if } P_1 < P_2 \end{cases} \quad (12)$$

Hydrogen consumption at the catalyst surface accounts for the flux of hydrogen leaving the anode channel into the GDL

$$W_{H_2,an,GDL} = -\frac{i_{st}}{2F} M_{H_2} A_{FC}. \quad (16)$$

The combined liquid and vapor flux entering the GDL from the channel  $W_{w,an,GDL}$  is found using Eq. (9). Nitrogen permeation across the membrane, as a function of the channel partial pressures of nitrogen,

$$W_{N_2,an,GDL} = \frac{k_{N_2,perm} M_{N_2} A_{FC}}{t_{mb}} (P_{N_2,ca,ch} - P_{N_2,an,ch}), \quad (17)$$

where  $k_{N_2,perm}(T_{st}, \lambda_{mb})$ , is a function of temperature and membrane water content from [2]. In this study, the parameter is fixed at  $k_{N_2,perm} = 1.5 \times 10^{-14} \text{ mol m}^{-1} \text{ s}^{-1} \text{ Pa}^{-1}$ . The partial pressures of each gas can be calculated from the mass using the ideal gas law,  $P_{N_2,an,ch} = m_{N_2,an,ch} R T_{st} / (M_{N_2} V_{an,ch})$ .

The individual gas species flows leaving the channel can be calculated from the total flow through the outlet orifice by multiplying with the binary control signal  $u$  and the mass fraction,

$$\begin{bmatrix} W_{H_2,an,out} \\ W_{N_2,an,out} \\ W_{w,an,out} \end{bmatrix} = u x_j W_{tot,an,out} \quad (18)$$

where  $W_{tot,an,out}$  is given by Eq. (12) with subscript  $j = 1$  corresponding to the anode channel when  $P_1 = P_{an,ch} \geq P_2 = P_{an,ko}$  and  $j = 2$ , otherwise indicating back-flow. When liquid water is present in the anode channel, we assume that it can cover the outlet orifice, and the gas mixture parameters are replaced with those corresponding to liquid water in equation (12), until the liquid is cleared. i.e.,

$$x_1 = \begin{cases} [x_{H_2,an,ch}, x_{N_2,an,ch}, x_{v,an,ch}]^T, & m_{l,an,ch} = 0 \\ [0, 0, 1]^T, & m_{l,an,ch} > 0 \end{cases} \quad (19)$$

The total mass flow into and out of the fuel cell channel volumes is given by (12), where  $C_{turb} = 0.61$  is the dimensionless discharge coefficient under turbulent conditions,  $D_h$  is the hydraulic diameter,  $A$  is the area of the orifice,  $R_t = 9.33$  is the critical value from [20],  $\rho$  is the density of the gas,  $\nu = \mu/\rho$  is the kinematic viscosity, and  $P_1, P_2$  are the upstream and downstream pressures.

## REFERENCES

- [1] J. B. Siegel and A. G. Stefanopoulou, "Through the membrane & along the channel flooding in PEMFCs," in *American Control Conference, 2009. ACC '09.*, June 2009, pp. 2666–2671.
- [2] S. S. Kocha, J. D. Yang, and J. S. Yi, "Characterization of gas crossover and its implications in PEM fuel cells," *AIChE Journal*, vol. 52, no. 5, pp. 1916–1925, 2006.
- [3] E. A. Müller, F. Kolb, L. Guzzella, A. G. Stefanopoulou, and D. A. McKay, "Correlating nitrogen accumulation with temporal fuel cell performance," *Journal of Fuel Cell Science and Technology*, vol. 7, no. 2, p. 021013, 2010.
- [4] W. Baumgartner, P. Parz, S. Fraser, E. Wallner, and V. Hacker, "Polarization study of a PEMFC with four reference electrodes at hydrogen starvation conditions," *Journal of Power Sources*, vol. 182, no. 2, pp. 413–421, Aug. 2008.
- [5] P. Rodatz, A. Tsukada, M. Mladek, and L. Guzzella, "Efficiency Improvements by Pulsed Hydrogen Supply in PEM Fuel Cell Systems," in *Proceedings of IFAC 15th World Congress*, 2002.
- [6] D. A. McKay, J. B. Siegel, W. Ott, and A. G. Stefanopoulou, "Parameterization and prediction of temporal fuel cell voltage behavior during flooding and drying conditions," *Journal of Power Sources*, vol. 178, no. 1, pp. 207–222, Mar. 2008.
- [7] G. Ripaccioli, J. B. Siegel, A. G. Stefanopoulou, and S. Di Cairano, "Derivation and simulation results of a hybrid model predictive control for water purge scheduling in a fuel cell," in *2nd Annual Dynamic Systems and Control Conference*, Hollywood, CA, USA, October 12–14 2009.
- [8] J. B. Siegel, D. A. McKay, A. G. Stefanopoulou, D. S. Hussey, and D. L. Jacobson, "Measurement of Liquid Water Accumulation in a PEMFC with Dead-Ended Anode," *Journal of The Electrochemical Society*, vol. 155, no. 11, pp. B1168–B1178, 2008.
- [9] J. B. Siegel, D. A. McKay, and A. G. Stefanopoulou, "Modeling and validation of fuel cell water dynamics using neutron imaging," in *Proc. American Control Conference*, 11–13 June 2008, pp. 2573–2578.
- [10] K. Promislow, P. Chang, H. Haas, and B. Wetton, "Two-Phase Unit Cell Model for Slow Transients in Polymer Electrolyte Membrane Fuel Cells," *Journal of The Electrochemical Society*, vol. 155, no. 7, pp. A494–A504, 2008.
- [11] J. B. Siegel, S. Yesilyurt, and A. G. Stefanopoulou, "Extracting Model parameters and Paradigms from Neutron Imaging of Dead-Ended Anode Operation," in *Proceedings of FuelCell2009 Seventh International Fuel Cell Science, Engineering and Technology Conference*, 2009.
- [12] B. A. McCain, A. G. Stefanopoulou, and I. V. Kolmanovsky, "On the dynamics and control of through-plane water distributions in PEM fuel cells," *Chemical Engineering Science*, vol. 63, no. 17, pp. 4418–4432, Sept. 2008.
- [13] S. Basu, C.-Y. Wang, and K. S. Chen, "Phase change in a polymer electrolyte fuel cell," *Journal of The Electrochemical Society*, vol. 156, no. 6, pp. B748–B756, 2009.
- [14] S. Ge, B. Yi, and P. Ming, "Experimental Determination of Electro-Osmotic Drag Coefficient in Nafion Membrane for Fuel Cells," *Journal of The Electrochemical Society*, vol. 153, no. 8, pp. A1443–A1450, 2006.
- [15] S. Ge, X. Li, B. Yi, and I.-M. Hsing, "Absorption, Desorption, and Transport of Water in Polymer Electrolyte Membranes for Fuel Cells," *Journal of The Electrochemical Society*, vol. 152, no. 6, pp. A1149–A1157, 2005.
- [16] T. Springer, T. Zawodzinski, and S. Gottesfeld, "Polymer Electrolyte Fuel Cell Model," *J. Electrochem. Soc.*, vol. 138, no. 8, pp. 2334–2341, 1991.
- [17] J. Hinatsu, M. Mizuhata, and H. Takenaka, "Water uptake of perfluorosulfonic acid membranes from liquid water and water vapor," *J. Electrochem. Soc.*, vol. 141, pp. 1493–1498, 1994.
- [18] J. Nam and M. Kaviany, "Effective diffusivity and water-saturation distribution in single and two-layer PEMFC diffusion medium," *Int. J. Heat Mass Transfer*, vol. 46, pp. 4595–4611, 2003.
- [19] A. Shah, G.-S. Kim, P. Sui, and D. Harvey, "Transient non-isothermal model of a polymer electrolyte fuel cell," *J. Power Sources*, vol. 163, no. 2, pp. 793–806, Jan. 2007.
- [20] W. Borutzky, B. Barnard, and J. Thoma, "An orifice flow model for laminar and turbulent conditions," *Simulation Modelling Practice and Theory*, vol. 10, no. 3–4, pp. 141–152, 2002.